A Coupled Petrophysical-Geophysical Model Demonstrates Velocity Dispersion in a Thin-bedded, Fluvial Reservoir*

Richard C. Odom[1]

Search and Discovery Article #40913 (2012)
Posted April 16, 2012

*Adapted from extended abstract prepared for poster presentation at AAPG Annual Convention and Exhibition, Long Beach, California, April 22-25, 2012,

[1]HWS Petrophysics, Arlington, Texas (odom@o-geosolutions.com)

Abstract

The Stratton Field 3-D seismic survey has been publicly available and widely distributed and studied for many years. The primary reservoir in this prolific gas play is the Frio Formation, a thin-bedded reservoir of fluvial origin. The two-mile by one-mile survey area has good well control with twenty one wells with well-logs; however, the correlation of fluvial reservoirs found in the wells to time-slices of the 3-D seismic has been enigmatic.

Using an interval of the upper-middle Frio formation that has good well coverage, good stratigraphic control and minimal tectonic deformation, a 3-dimensional statistical model was developed to search the 3-D seismic for correlation. The correlation of the well-logs to the VSP time-depth chart was very good; however, the positions of the targeted fluvial objects in the 3-dimensional search showed that the VSP time-depth chart was much faster than the time-depth positions in the 3-D seismic. The noted shifts between VSP and 3-D seismic were on the order of 18mS TWT (two-way time) shift in 500 feet; this translates to approximately a 90-foot targeting error. This is a very significant error when targeting the thin fluvial reservoir sands that are typically 30 to 60 feet thick.

The seismic velocities, wavelengths and bed distributions appear scalable to velocity dispersion described by forward modeling and experimental results. To test this hypothesis, a classifier was developed to identify beds based on three predominant facies: reservoir sands, tight sands and floodplain mudstones using the well log data. The bed-thickness distributions for the wells show a thin-layered reservoir with geometric scales where velocity dispersion is predicted.

These results have significant impacts in the proper handling and targeting of seismic data in reservoirs such as the Frio Formation:
1. Thin-bed velocity-dispersion is a potent effect in these types of reservoirs;
2. Lateral heterogeneity in dispersive parameters may require special consideration when targeting thin fluvial members.

3. Synthetic seismogram techniques, such as Weiner-Levinson wavelets, rely on linear statistical models and do not account for dispersion.
4. An improved time-depth chart is published for this section of the survey based on a linear relation to the target positions.

Introduction

A public domain seismic data set that covers the Frio formation in the Stratton field is available from The University of Texas Bureau of Economic Geology. The Stratton field is part of the prolific FR-4 gas play; the field is in Nueces County, near the city of Corpus Christi, Texas (Figure 1--location map).

At the location of the Stratton field, the Frio is part of the Gueydan fluvial system characterized by floodplains, channels and splay sands deposited at the ancient Rio Grande embayment. The Frio formed a thick progradational wedge deposited during a time with plentiful sediment supply and continued subsidence along the Gulf Coast; in the Stratton field the Frio deposits are approximately 3300 feet thick. Along with plentiful sediment, the river system was not well bounded by the coastal plain; this is expressed in the stratigraphic record by long periods of floodplain aggradation cyclically interrupted by river channels and splays wandering through the field.

The depositional model was originally drafted by Galloway (1982) and later updated by Kerr (1990) and Ambrose (2000). The channel-fill sands are typically 30 feet thick, often stacked and amalgamated laterally. These sands are bounded by silt and mud-rich floodplain deposits. Kerr (1990) describes the channel-fill facies as relatively straight pathways with low sinuosity that are typically 30+/- 15 feet thick and 2500 ±500 feet wide. A single splay is modeled as fan-shaped, but, because the splays are stacked, the changing depositional energy, accommodation space and crevasse location generate irregular shapes. Reservoir sands in the splay facies are thin and proximal to the channel; the splay complexes can be 20 +/- 10 feet thick and can extend 2 to 3 miles from the channel.

The data set covers a 1-mile by 2-mile area with 3-D seismic, also there are 21 wellbores with logs, and one well has a Vertical Seismic Profile (VSP). The project is supplied with a time-depth chart derived from the VSP survey. A section of the upper middle Frio from 5000 to 5800 depth was selected for this study. As discussed below, this section has minimal tectonic deformation and very tight stratigraphic controls; so, given the dense well spacing it is fairly straightforward to correlate the fluvial sequences from the well log data. Initial efforts in processing this data set by Hardage (1994) suggested a recipe of looking at seismic amplitude slices, but the correlation to well-to-well log correlations is poor.

Analysis of the synthetic seismic suggests problems with the time-depth chart. So, the initial research involved 3-dimensional searches for correlation over a broad window of time slices. The results from 3 different searches for reservoir targets demonstrate that the VSP time-depth chart is faster than the target locations in the 3-D seismic. The different frequency components of the 3-D seismic and the VSP lead to the hypothesis: There is significant velocity dispersion causing errors in the time-depth chart.

Stratigraphic Control

The stratigraphic column is bound by regional surfaces that are interpreted as erosional unconformities; at the base is the unconformity above the E41 sand; at the top is the unconformity below the C18 sand. This section can be identified by the gamma-ray log since the sediments contain 15 to 20% volcanic ash and glass (Kerr, 1991). The volcanic sediment raises the baseline on the gamma-ray log; also, depositional artifacts, possibly aeolian/lacustrine deposits, have created gamma-ray markers that can be used for well-to-well correlation.

The stratigraphic column builds at the rate of floodplain aggradation. The river channel incises the floodplain, and the channel fill is laterally accreted so the base and top of the channel roughly tie in time to the floodplain at the top of a specific channel. The timing of deposition gets convoluted as the channel stacks and amalgamates laterally, and the splays are interleaved with paleosols of the floodplains. The chronostratigraphic markers are the continuous floodplains; these layers of flooding surfaces mark the fluvial parasequence boundaries. The floodplains can be identified on the well logs using the resistivity response.

Armed with the chronostratigraphic markers from the gamma ray and the parasequence boundaries from the floodplains, the well-log data can be tightly constrained and flattened in depth. Figure 2 is an isopach of the column thickness; we can note the study area is basically flat, with extremes of 17 feet of sediment growth in the western and south-eastern edges of the survey.

Correlation of Seismic to Well-Log Data

The synthetic seismogram from the well logs using a zero-phased wavelet did not have a good match to the 3-D trace. You could force a match with a Wiener-Levinson filter, but this does not add accuracy to our time-depth targeting problem. However, it is analytic on the quality of the depth match. The matching filter is shown in Figure 3; the response shows energy smeared over a broad interval (i.e., more than 80 milliseconds).

Figure 4 is a log plot of the seismic trace, the VSP, and open-hole logs. There is a good correlation of the VSP and the open-hole logs. There were no sonic logs in the data set. In the 3rd track is an overlay of Delta Time from the VSP and Delta Time correlated from the open-hole logs using neural network analysis (IPNNL 2004b). In the 5th track is the seismic trace, the big peak at 5040 is a prominent reflector that can be tracked across the study volume. Given the Wiener-Levinson Wavelet, the rocks, and the VSP response, it seems logical to tie this reflector to the c18 sand at 4940. Thus the well logs were flattened to c18 and the seismic was flattened to this reflector, the original time-depth values of well 9 are still intact.

Fluvial Target Search

Given a flat and consistent study volume, a scoring model was developed based on the fluvial members noted in a specific parasequence (i.e., river channel sands, tight-layered splays and levees, floodplains) on the well logs. The wells were divided into 12 training wells and 6

testing wells and seismic traces over a 50-millisecond window near the wellbores were used as training data for a neural network. The trained network was used to process a classification map of the entire survey. The seismic slice that scored most like the successful network was selected as "most potent".

Given successful network training we can dissect the training data for potency using a sub-setting algorithm. The GIGO software (Li, 2006a, 2006b) from the Image Processing and Neural Networks Lab at University of Texas at Arlington performs the sub-setting and evaluations of the training data automatically. The training data is segregated into clusters, and the error calculation for a given subset uses the corresponding rows and columns of the auto- and cross-correlation matrices for each cluster. The output from GIGO ranks which points on the trace (i.e., time-slice intersections) are the most important in correctly classifying the fluvial element.

The results from search scoring and GIGO sub-setting were fairly consistent on the pick of "most potent slice" for the three target hunts; the most potent slice is plotted versus time offset in Figure 5. More information on the search recipe and results can be found in Odom (2009). Of importance in this work is establishing the time-depth error; indeed, we would not need this elaborate search process if we could target the seismic slice that is most credible in describing the fluvial architectural element.

Dispersion Hypothesis

Perusal of Figure 5 leads to the conclusion that the velocity of the 3-D seismic signal is much slower than the velocity of the VSP signal. Figure 6, from Rio (1996), diagrams the effects of velocity dispersion on laboratory experiments using stacked layers. Similar results can be found in the literature on forward modeling of layered media. Given that the 3-D wavelength will be longer than the VSP, we are led to the hypothesis that the targeting error is related to velocity dispersion.

To test the hypothesis, bed-thickness counts were generated from the well logs. Using a neural network classifier (IPNNL 2004b) as diagrammed in Figure 7, the formations were sorted into three classes:

- Floodplain deposits: fine grained with paleosols, loess and lacustrine layers. 1
- Tight sandstones: feldspathic litharenites, fine-grained, lithic glass fragments, clay cement. 1
- Reservoir sandstones: feldspathic litharenites, coarser grained; lithic fragments are glass and carbonates, leached calcite cement.

The mineralogical composition is similar in all three classes, the main distinctions between the facies are grain size and diagenetic alteration (Grigsby, 1991). For example, the reservoir sands are coarser grained and the porosity/permeability of the reservoir sands has been enhanced by secondary leaching (Loucks, 1977).

Figure 8 shows the bed thickness count as a percentage of the interval (i.e., linear feet of a specific thickness). Using the bed count, nominal ranges for parameters, and the graph from Rio (1996) would generate an estimate that the 3-D velocity is 20 to 30% slower than the VSP;

Figure 5 shows more than 40% was observed. This is of course a very naïve analysis, but, of note, the observed error scales well with forward modeling.

Conclusions

A coupled petrophysical-geophysical model demonstrates that velocity dispersion is significant error in targeting thinly layered reservoirs such as the Frio formation of south Texas. In Figure 9 is a table of time to depth over the study volume. Of note in these types of reservoirs:

- Targeting thin fluvial reservoirs requires that the time-depth accuracy be tightly constrained;
- In reservoirs similar to the Frio, the VSP may not be an accurate time-depth benchmark;
- Lateral heterogeneity requires localized flattening to maintain depth accuracy; 1
- Wiener-Levinson wavelets or other linear statistical models are good with multiples and mixed-phase additive noise but are not structured for dispersion between the data sets.

References

Galloway, W.E., 1982, Depositional architecture of Cenozoic gulf coastal plain fluvial systems: B.E.G. Geological circular 82-5, reprinted from SEPM Special Publication No.31.

Grigsby, J.D., and D.R. Kerr, 1991, Diagenetic variability in middle Frio reservoirs (Oligocene), Seeligson and Stratton fields, south Texas: Transactions of the GCAGS, v. 41, p. 308-319.

Hardage, B A., R.A. Levey, V. Pendleton, J. Simmons, and R. Edson, 1994, A 3-D seismic case history evaluating fluvially deposited thin-bed reservoirs in a gas-producing property: Geophysics, v. 59/11, p. 1650-1665.

Kerr, D.R., and J.D. Grigsby, 1991, Recognition and implications of volcanic glass detritus in the fluvial deposits of the middle Frio formation, south Texas: Transactions of the GCAGS, v. XLI, p. 353-358.

Kerr, D.R., and L.A. Jirik, 1990, Fluvial architecture and reservoir compartmentalization in the Oligocene middle Frio formation, south Texas: Transactions of the GCAGS, v. XL, p. 373-380.

Li, J., M.T. Manry, P. Narasimha, and C. Yu, 2006a, Feature selection using a piecewise linear network: IEEE Transactions on Neural Networks, v. 17/5, p. 1101-1115.

Li, J., J. Yao, R.M. Summers, N. Petrick, M.T. Manry, and A.K. Hara, 2006b, An efficient feature selection algorithm for computer-aided

polyp detection: special issue of the International Journal on Artificial Intelligence Tools (IJAIT), v. 15/6, p. 893-915.

Loucks, R.G., D.G. Bebout, and W.E. Galloway, 1977, Relationship of porosity formation and preservation to sandstone consolidation history – Gulf Coast lower tertiary Frio formation: Geological Circular 77-5, reprinted from transactions of the GCAGS, v. 27, p. 109-120.

Odom, R.C., 2009, Seismic inversion in fluvial reservoirs: Building a geologic model-based inversion for the Stratton Field 3d survey: Master's Thesis, University of Texas at Arlington, 170 p.

Rio, P., T. Mukerji, G. Mavko, and D. Marion, 1996, Velocity dispersion and upscaling in a laboratory-simulated VSP: Geophysics v. 61/2, p. 584-593.

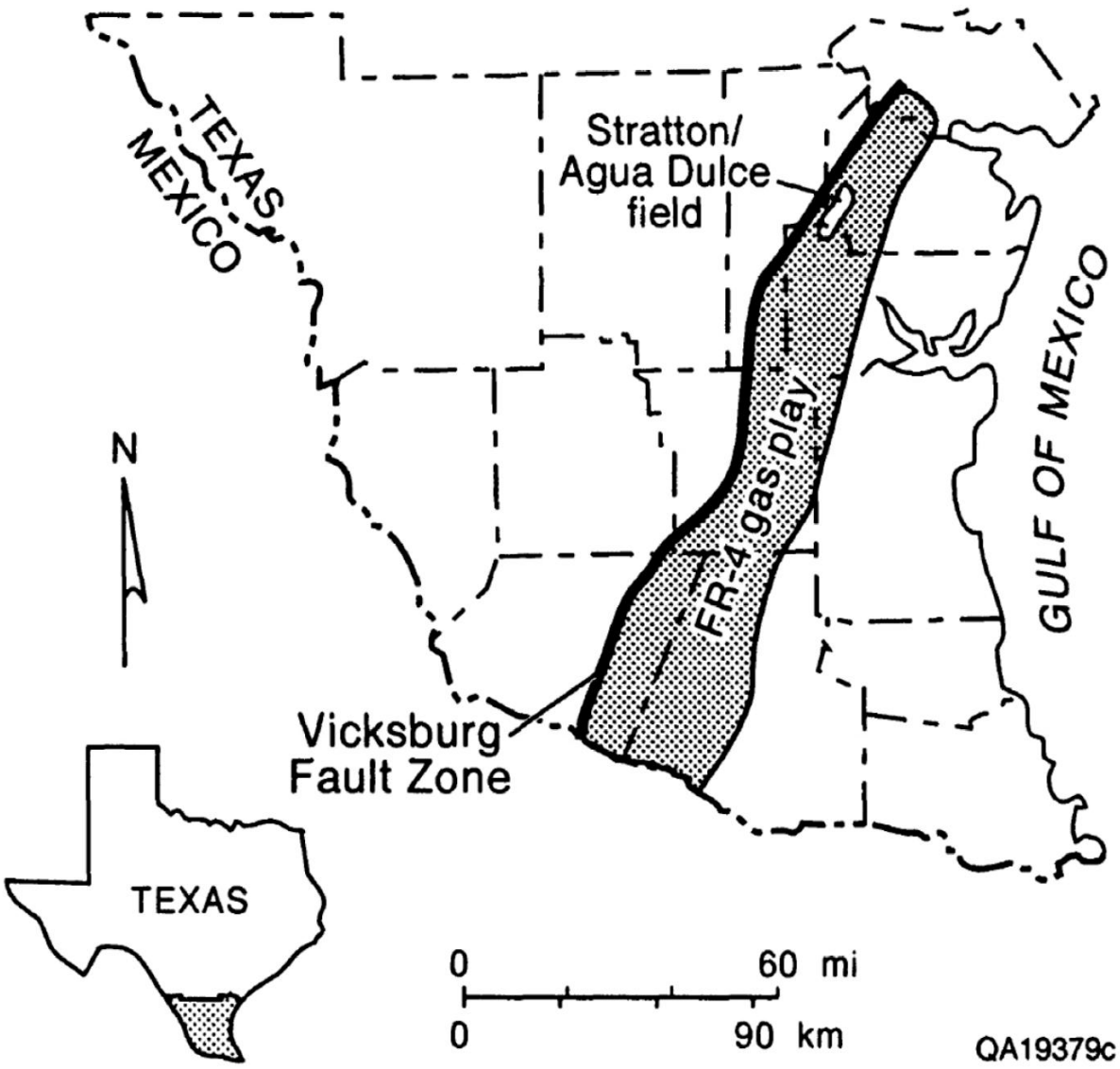

Figure 1. Location map of Stratton field in south Texas.

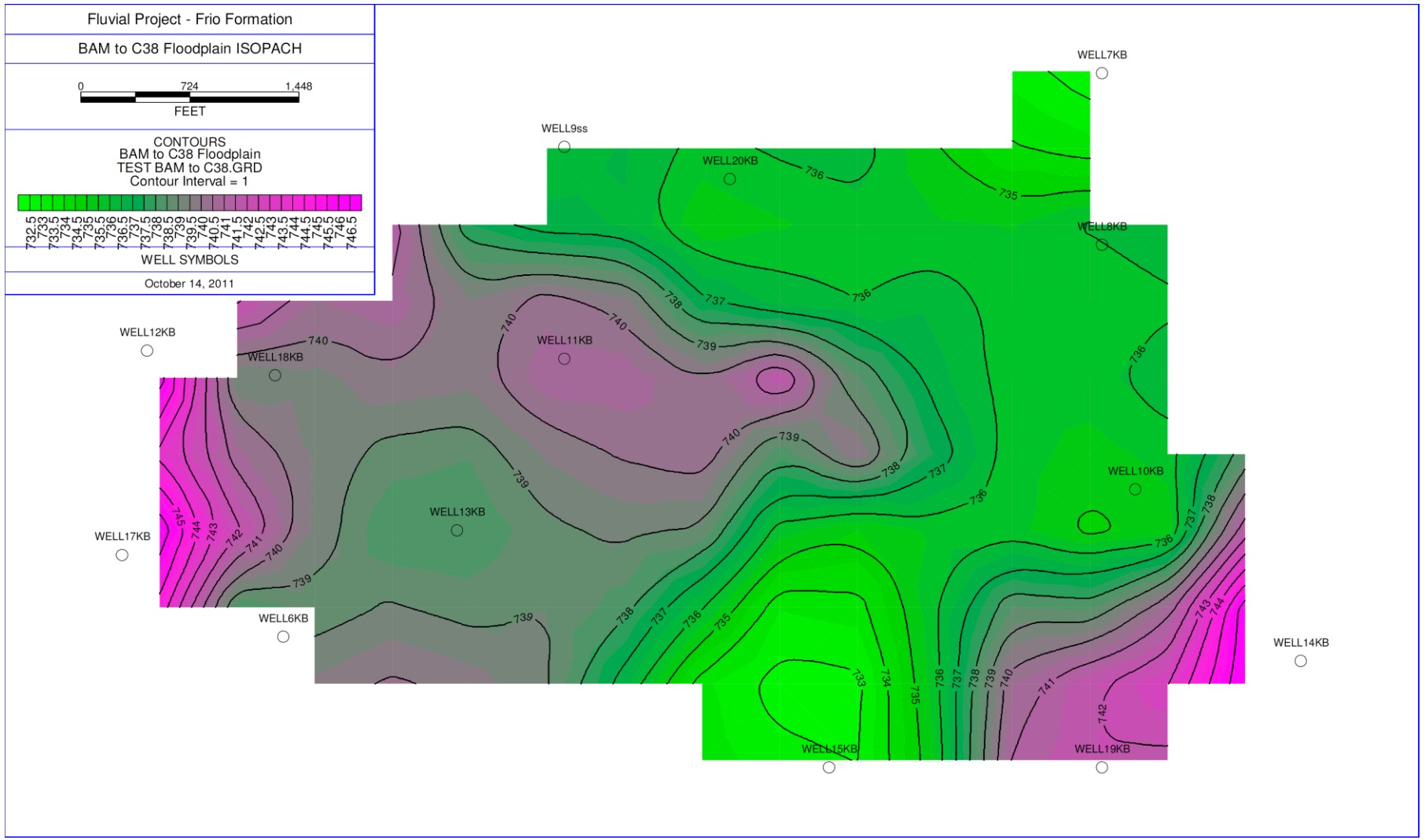

Figure 2. Isopach map of stratigraphic column, basal ash marker to c38 floodplain.

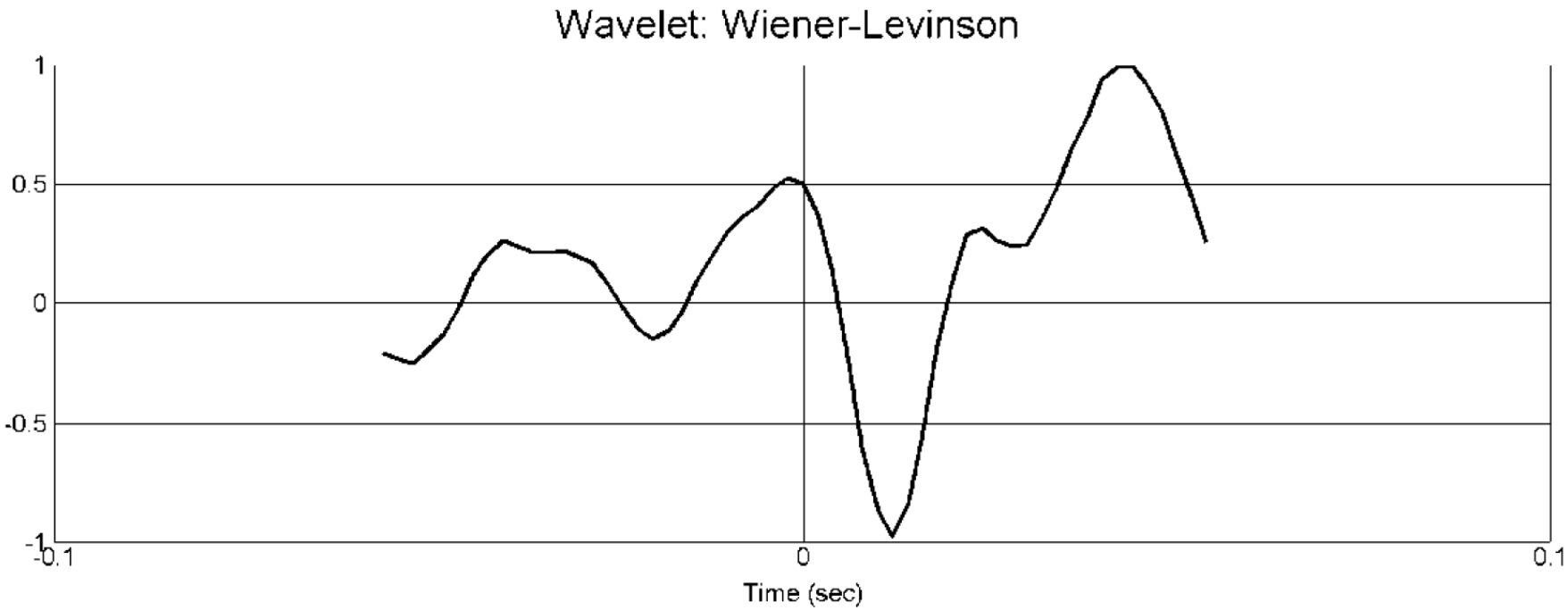

Figure 3.Wiener-Levinson Wavelet for synthetic seismogram over study volume.

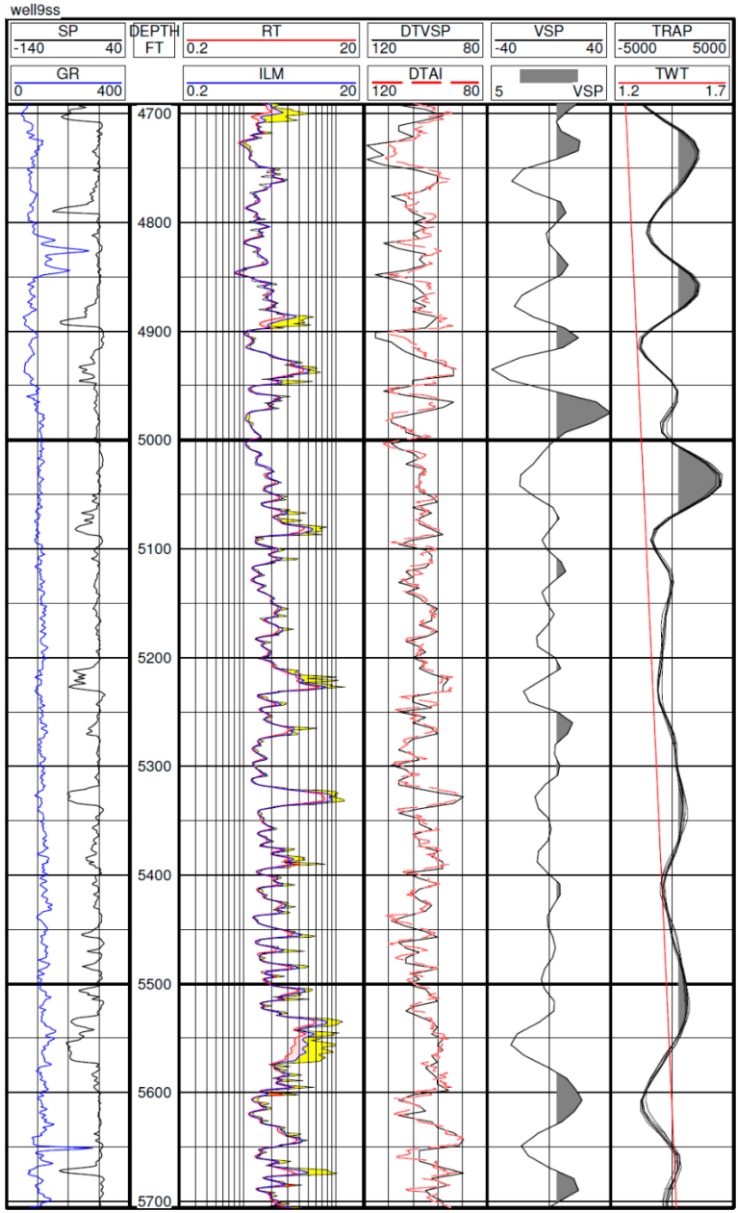

Figure 4.Well Stratton # 9 (well 9): well logs, track one has open hole gamma ray and SP (spontaneous potential); track 2 is triple resistivity; track 3 is delta time from VSP and open hole; track 4 is the VSP trace; in track 5 are seismic traces from the 3-D survey.

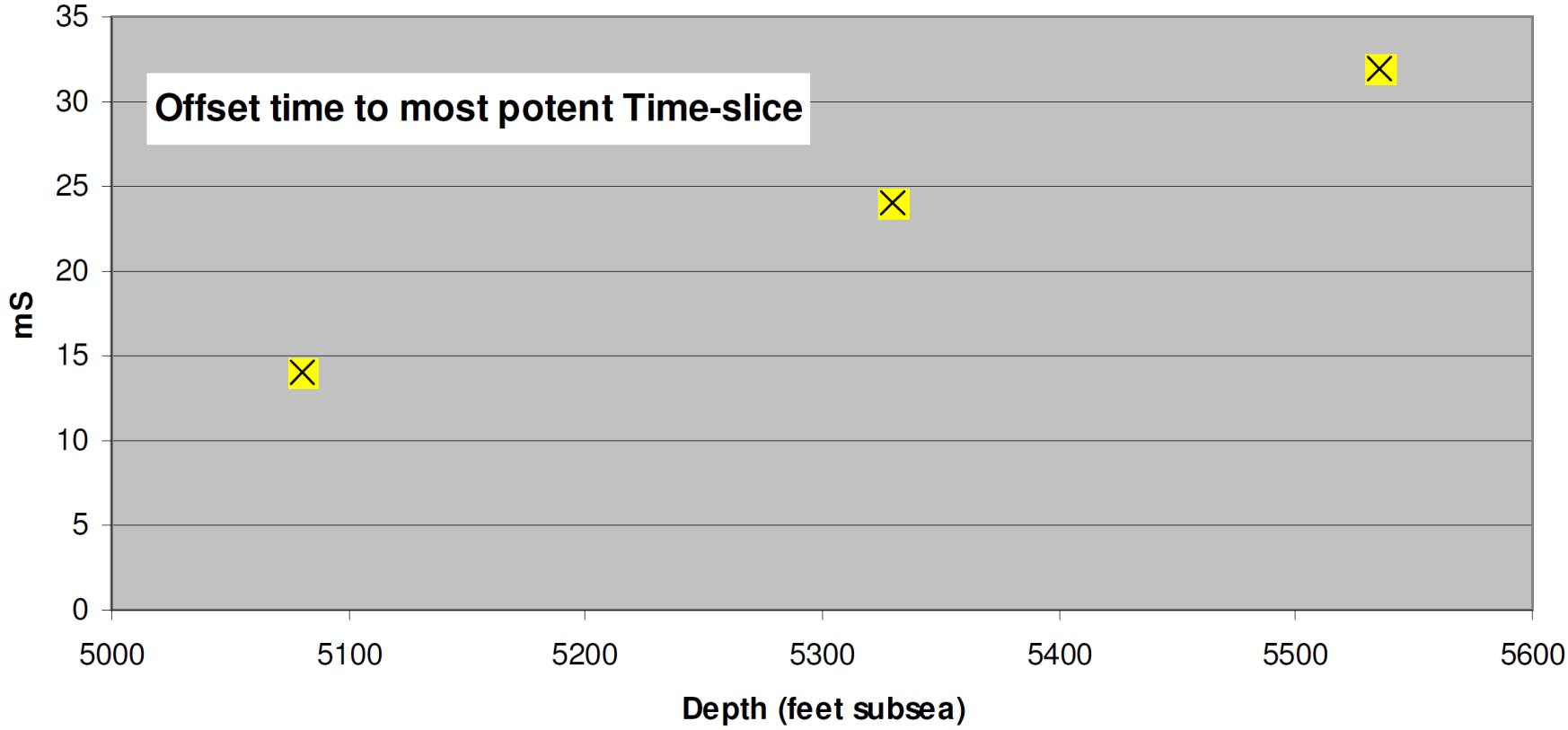

Figure 5. The locations of targets: depth versus offset time.

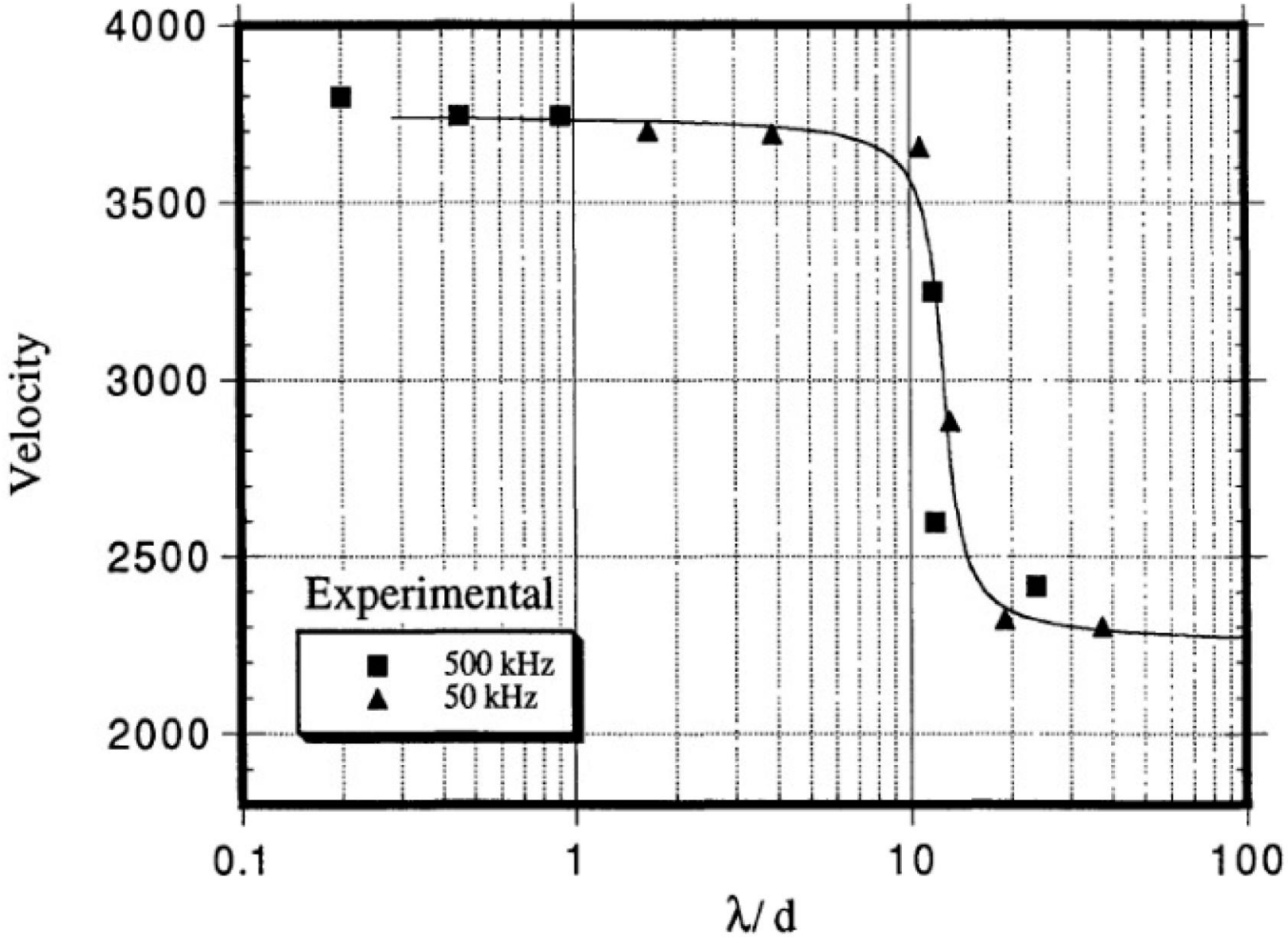

Figure 6. Illustration of the concept of frequency-dependent velocity dispersion in thin-bedded sequences. The scale l/d is the ratio of wavelength to bed thickness (from Rio (1996 (Figure)).

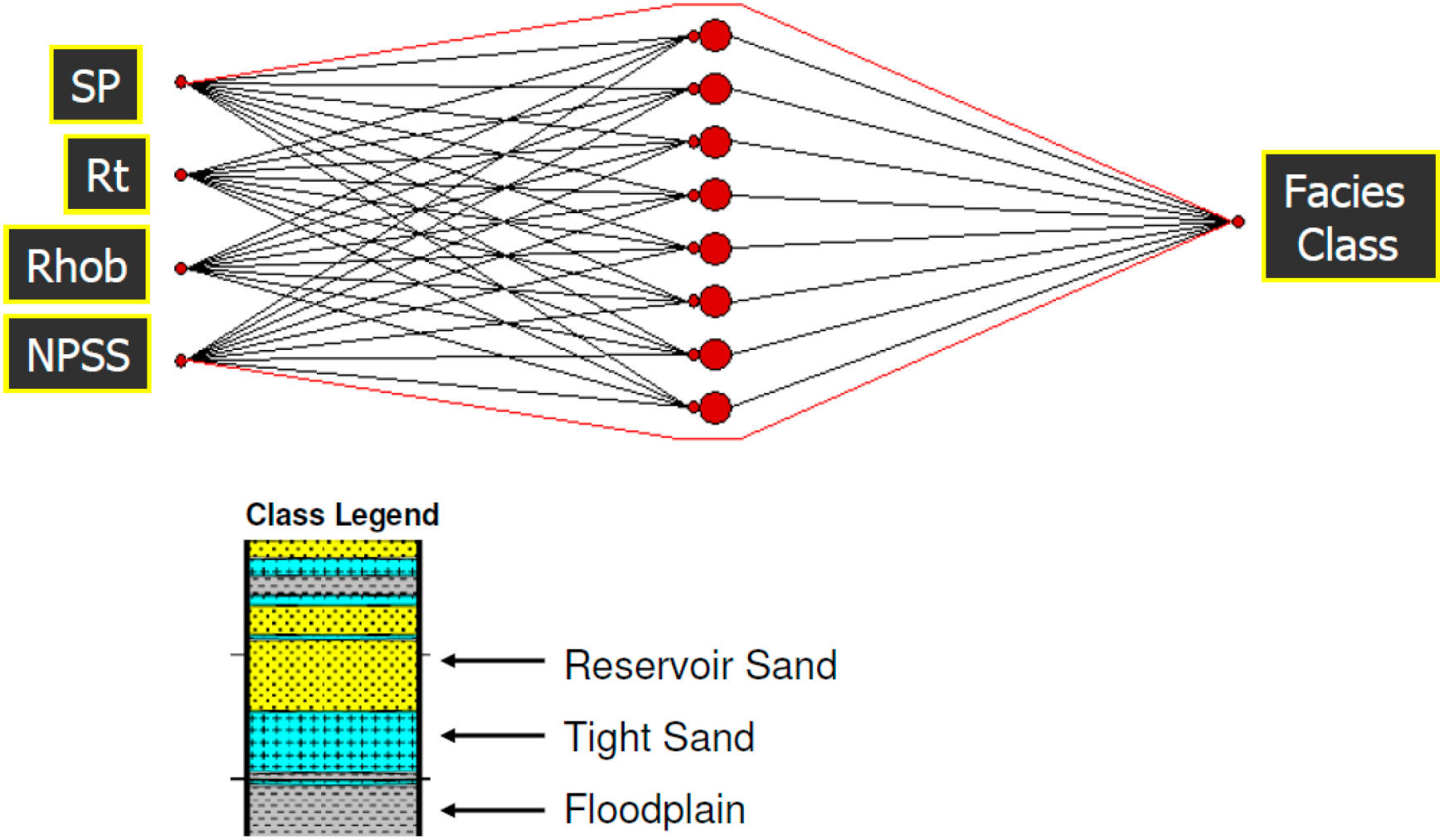

Figure 7. Formation classifier neural network to make bed thickness classes.

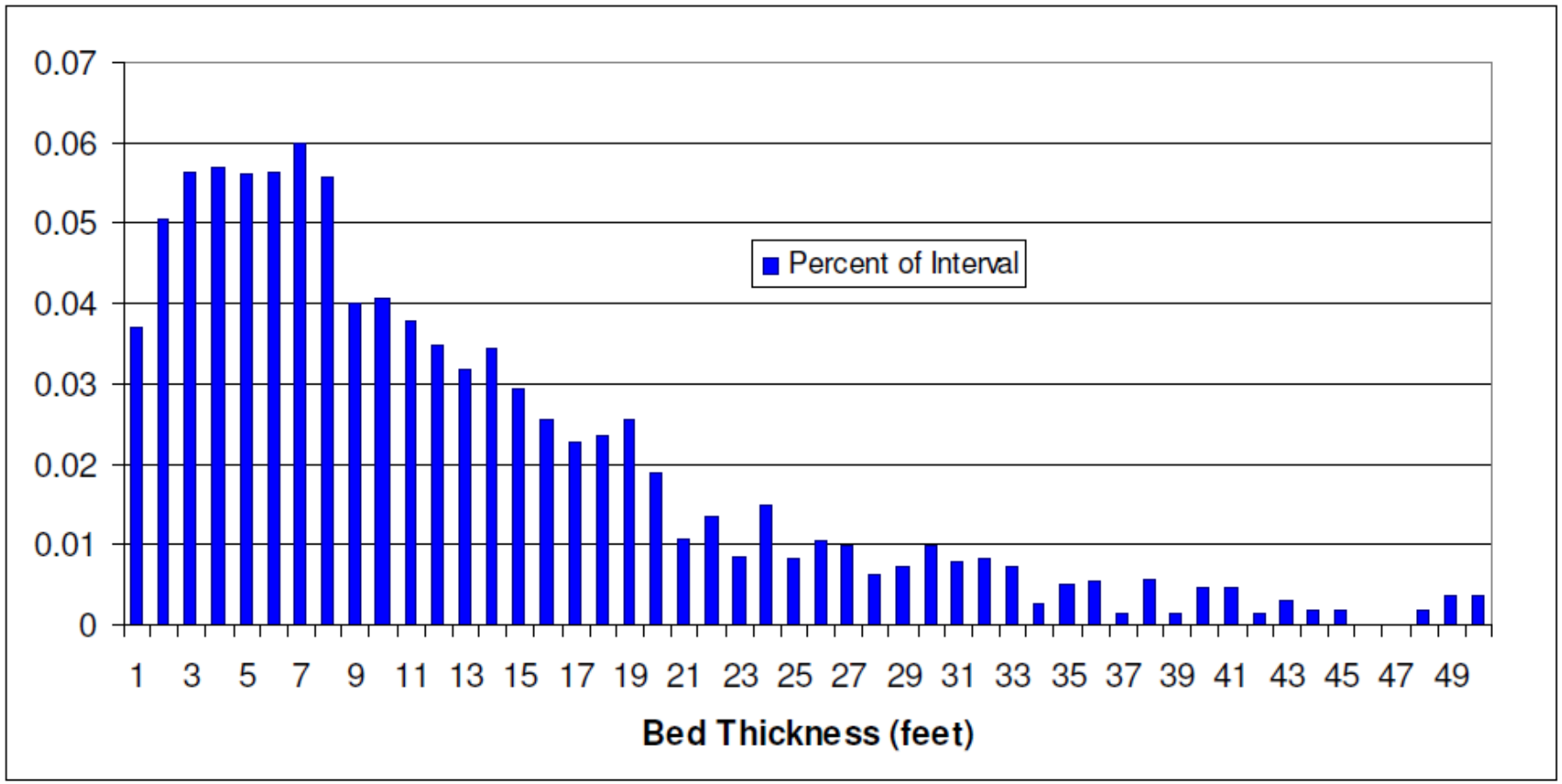

Figure 8.Bed-thickness distribution.

Depth	TWT VSP	TWT 3-D	Depth	TWT VSP	TWT 3-D	Depth	TWT VSP	TWT 3-D
5000.7	1.301	1.333538	5264.1	1.355	1.385428	5537.1	1.41	1.439209
5005.9	1.302	1.334562	5269.1	1.356	1.386413	5542	1.411	1.440174
5011	1.303	1.335567	5274.3	1.357	1.387437	5547.1	1.412	1.441179
5016	1.304	1.336552	5279.4	1.358	1.388442	5552.1	1.413	1.442164
5020.3	1.305	1.337399	5284.5	1.359	1.389447	5556.8	1.414	1.44309
5024.6	1.306	1.338246	5289.4	1.36	1.390412	5561.3	1.415	1.443976
5029.1	1.307	1.339133	5294.6	1.361	1.391436	5566	1.416	1.444902
5033.7	1.308	1.340039	5299.6	1.362	1.392421	5571	1.417	1.445887
5038.4	1.309	1.340965	5304.3	1.363	1.393347	5576.2	1.418	1.446911
5043.3	1.31	1.34193	5309.2	1.364	1.394312	5580.8	1.419	1.447818
5048.6	1.311	1.342974	5314.2	1.365	1.395297	5585.5	1.42	1.448744
5054.1	1.312	1.344058	5319	1.366	1.396243	5590.4	1.421	1.449709
5059.6	1.313	1.345141	5324	1.367	1.397228	5595.1	1.422	1.450635
5064.4	1.314	1.346087	5328.9	1.368	1.398193	5599.8	1.423	1.451561
5069.2	1.315	1.347032	5334	1.369	1.399198	5605	1.424	1.452585
5073.6	1.316	1.347899	5339.4	1.37	1.400262	5609.8	1.425	1.453531
5078.3	1.317	1.348825	5344.7	1.371	1.401306	5614.7	1.426	1.454496
5083.8	1.318	1.349909	5350	1.372	1.40235	5619.4	1.427	1.455422
5089.1	1.319	1.350953	5354.8	1.373	1.403296	5624.4	1.428	1.456407
5094	1.32	1.351918	5359.6	1.374	1.404241	5629.5	1.429	1.457412
5098.5	1.321	1.352805	5364.7	1.375	1.405246	5634.7	1.43	1.458436
5103	1.322	1.353691	5369.3	1.376	1.406152	5639.5	1.431	1.459382
5107.7	1.323	1.354617	5374.3	1.377	1.407137	5644.2	1.432	1.460307
5112.4	1.324	1.355543	5379.1	1.378	1.408083	5649.1	1.433	1.461273
5117.4	1.325	1.356528	5384.2	1.379	1.409087	5654.2	1.434	1.462277
5121.9	1.326	1.357414	5389.4	1.38	1.410112	5659.4	1.435	1.463302
5126.5	1.327	1.358321	5394.2	1.381	1.411057	5664.5	1.436	1.464307
5131.3	1.328	1.359266	5398.9	1.382	1.411983	5669.8	1.437	1.465351
5136.2	1.329	1.360231	5403.5	1.383	1.41289	5675	1.438	1.466375
5140.9	1.33	1.361157	5408.3	1.384	1.413835	5680.3	1.439	1.467419
5145.9	1.331	1.362142	5413.2	1.385	1.4148	5685.4	1.44	1.468424
5150.8	1.332	1.363108	5417.7	1.386	1.415687	5690.6	1.441	1.469448
5155.7	1.333	1.364073	5422.4	1.387	1.416613	5695.6	1.442	1.470433
5160.6	1.334	1.365038	5427.2	1.388	1.417558	5700.7	1.443	1.471438
5165.5	1.335	1.366004	5431.8	1.389	1.418465	5705.9	1.444	1.472462
5170.6	1.336	1.367008	5436.4	1.39	1.419371	5711.1	1.445	1.473487
5175.8	1.337	1.368033	5441.5	1.391	1.420376	5716.5	1.446	1.474551
5180.6	1.338	1.368978	5447.2	1.392	1.421498	5721.3	1.447	1.475496
5185.7	1.339	1.369983	5452.7	1.393	1.422582	5725.9	1.448	1.476402
5190.6	1.34	1.370948	5457.6	1.394	1.423547	5730.8	1.449	1.477368
5195.5	1.341	1.371914	5462.2	1.395	1.424453	5735.8	1.45	1.478353
5200.6	1.342	1.372918	5467.1	1.396	1.425419	5740.4	1.451	1.479259
5205.9	1.343	1.373962	5472	1.397	1.426384	5745.5	1.452	1.480264
5210.7	1.344	1.374908	5477.1	1.398	1.427389	5750.7	1.453	1.481288
5215.3	1.345	1.375814	5481.9	1.399	1.428334	5756.2	1.454	1.482371
5220.3	1.346	1.376799	5486.8	1.4	1.4293	5761.9	1.455	1.483494
5225.4	1.347	1.377804	5491.7	1.401	1.430265	5767.5	1.456	1.484598
5230.5	1.348	1.378809	5496.9	1.402	1.431289	5772.4	1.457	1.485563
5235.5	1.349	1.379794	5502	1.403	1.432294	5777.3	1.458	1.486528
5240.2	1.35	1.380719	5507.3	1.404	1.433338	5782.2	1.459	1.487493
5245	1.351	1.381665	5512.6	1.405	1.434382	5787.5	1.46	1.488538
5249.6	1.352	1.382571	5517.3	1.406	1.435308	5793.2	1.461	1.48966
5254.5	1.353	1.383537	5522.2	1.407	1.436273	5798.3	1.462	1.490665
5259.2	1.354	1.384462	5527.4	1.408	1.437298	5803.7	1.463	1.491729

Figure 9. Time-depth chart for #-D I study volume.